J|A|C|S
ARTICLES
Published on Web 03/25/2004

Catalysis with TiO_2/Gold Nanocomposites. Effect of Metal Particle Size on the Fermi Level Equilibration

Vaidyanathan Subramanian, Eduardo E. Wolf, and Prashant V. Kamat*

Contribution from the Notre Dame Radiation Laboratory and Department of Chemical & Biomolecular Engineering, University of Notre Dame, Notre Dame, Indiana 46556

Received December 4, 2003; E-mail: pkamat@nd.edu

Abstract: Photoexcited semiconductor nanoparticles undergo charge equilibration when they are in contact with metal nanoparticles. Such a charge distribution has direct influence in dictating the energetics of the composite by shifting the Fermi level to more negative potentials. The transfer of electrons to Au nanoparticles has now been probed by exciting TiO_2 nanoparticles under steady-state and laser pulse excitation. Equilibration with the C_{60}/C_{60}^- redox couple provides a means to determine the apparent Fermi level of the TiO_2−Au composite system. The size-dependent shift in the apparent Fermi level of the TiO_2−Au composite (20 mV for 8-nm diameter and 40 mV for 5-nm and 60 mV for 3-nm gold nanoparticles) shows the ability of Au nanoparticles to influence the energetics by improving the photoinduced charge separation. Isolation of individual charge-transfer steps from UV-excited TiO_2 → Au → C_{60} has provided mechanistic and kinetic information on the role of metal in semiconductor-assisted photocatalysis and size-dependent catalytic activity of metal−semiconductor nanocomposites.

Introduction

Semiconductor−metal nanocomposites have been widely employed in photocatalysis.[1−12] Where as the metal in contact with the semiconductor greatly enhances the overall photocatalytic efficiency, the role it plays in dictating the interfacial charge-transfer processes is yet to be understood fully. A better understanding of the energetics of such nanocomposite systems is important for tailoring the properties of next-generation nanodevices. Scheme 1 illustrates the mediating role of noble metals in storing and shuttling photogenerated electrons from the semiconductor to an acceptor in a photocatalytic process.

Semiconductor−metal composites have been suggested for a wide variety of applications.[7,13−18] Earlier investigations on semiconductor−metal composites have revealed that deposition of metal on semiconductor enhances the efficiency of photocatalytic redox processes.[19−23] Recently, we reported a higher yield of thiocyanate radical formation in the presence of gold deposited on TiO_2.[9] Composite films based on TiO_2 and metal (Au, Pt, Ir) nanostructures have shown higher photocurrent and photovoltage and increasing charge separation.[24−27]

Scheme 1. Fermi Level Equilibration in a Semiconductor−Metal Nanocomposite System

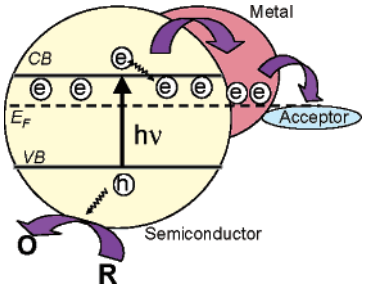

Electron transfer between photoexcited semiconductor and metal is an important phenomenon in photocatalysis. TiO_2 nanoparticles modified with precious metals have been extensively employed in photocatalytic water-splitting reactions.[28−30]

(1) Kraeutler, B.; Bard, A. J. *J. Am. Chem. Soc.* **1978**, *100*, 4317.
(2) Nosaka, Y.; Norimatsu, K.; Miyama, H. *Chem. Phys. Lett.* **1984**, *106*, 128.
(3) Baba, R.; Nakabayashi, S.; Fujishima, A.; Honda, K. *J. Phys. Chem.* **1985**, *89*, 1902.
(4) Heller, A. *Nato Asi Ser., Ser. C* **1986**, *15*.
(5) Kalyanasundaram, K.; Graetzel, M.; Pelizzetti, E. *Coord. Chem. Rev.* **1986**, *69*, 57.
(6) Henglein, A. *Chem. Rev.* **1989**, *89*, 1861.
(7) Kamat, P. V. *Pure Appl. Chem.* **2002**, *74*, 1693.
(8) Kamat, P. V. *J. Phys. Chem. B* **2002**, *106*, 7729.
(9) Kamat, P. V.; Flumiani, M.; Dawson, A. *Colloids Surf., A* **2002**, *202*, 269.
(10) Kamat, P. V.; Meisel, D. *Curr. Opin. Colloid Interface Sci.* **2002**, *7*, 282.
(11) Zhang, J. Z. *Acc. Chem. Res.* **1997**, *30*, 423.
(12) George Thomas, K.; Kamat, P. V. *Acc. Chem. Res.* **2003**, *36*, 888.
(13) Mulvaney, P.; Grieser, F.; Meisel, D. *Langmuir* **1990**, *6*, 567.
(14) Pastoriza-Santos, I.; Koktysh, D. S.; Mamedov, A. A.; Giersig, M.; Kotov, N. A.; Liz-Marzan, L. M. *Langmuir* **2000**, *16*, 2731.
(15) Zhang, J.; Coombs, N.; Kumacheva, E.; Lin, Y.; Sargent, E. H. *Adv. Mater.* **2003**, *15*, 1756.
(16) Willner, I.; Willner, B. *Pure Appl. Chem.* **2001**, *73*, 535.
(17) Zayats, M.; Kharitonov, A. B.; Pogorelova, S. P.; Lioubashevski, O.; Katz, E.; Willner, I. *J. Am. Chem. Soc.* **2003**, *125*, Web release.
(18) Kamat, P. V.; Meisel, D. *C. R. Chimie* **2003**, *6*, 999.
(19) Nosaka, Y.; Ishizuka, Y.; Miyama, H. *Ber. Bunsen-Ges. Phys. Chem.* **1986**, *90*, 1199.
(20) Henglein, A. *Ber. Bunsen-Ges. Phys. Chem.* **1995**, *99*, 903.
(21) Ikeda, S.; Sugiyama, N.; Pal, B.; Marci, G.; Palmisano, L.; Noguchi, H.; Uosaki, K.; Ohtani, B. *Phys. Chem. Chem. Phys.* **2001**, *3*, 267.
(22) Dawson, A.; Kamat, P. V. *J. Phys. Chem. B* **2001**, *105*, 960.
(23) Szabo-Bardos, E.; Czili, H.; Horvath, A. *J. Photochem. Photobiol., A* **2003**, *154*, 195.
(24) Nakato, Y.; Shioji, M.; Tsubomura, H. *Chem. Phys. Lett.* **1982**, *90*, 453.
(25) Nakato, Y.; Ueda, K.; Yano, H.; Tsubomura, H. *J. Phys. Chem.* **1988**, *92*, 2316.
(26) Chandrasekharan, N.; Kamat, P. V. *J. Phys. Chem. B* **2000**, *104*, 10851.
(27) Subramanian, V.; Wolf, E.; Kamat, P. V. *J. Phys. Chem. B* **2001**, *105*, 11439.
(28) Bard, A. J.; Fox, M. A. *Acc. Chem. Res.* **1995**, *28*, 141.

A direct correlation between the work function of the metal and the photocatalytic activity for the generation of NH_3 from azide ions has been made for metallized TiO_2 systems.[2] Recent studies have shown that metal or metal ion doped semiconductor composites exhibit shift in the Fermi level to more negative potentials.[31−34] Such a shift in the Fermi level improves the energetics of the composite system and enhances the efficiency of interfacial charge-transfer process. The unusual property of gold nanoparticles to undergo quantized charging makes them a unique candidate to achieve Fermi-level equilibration.[35] Platinum metal, on the other hand, introduces ohmic contact facilitating a quick transfer of electrons to the electrolyte.[32]

Electrochemical,[36−38] photochemical,[32,39] and spectroelectrochemical[40,41] experiments have shown that the gold nanoparticles capped with organic molecules exhibit unusual redox activity by readily accepting electrons from a suitable donor or an electrode. If such metal particles come in contact with a charged semiconductor nanostructure or nanoparticle, the Fermi levels of the two systems equilibrate. One factor that can potentially influence the electronic properties of the nanocomposite is the size of the metal particle. For example, Haruta and co-workers[42,43] demonstrated that gold nanoparticles in the 2−5-nm range show unusually high catalytic activities. Similarly, Goodman and co-workers have demonstrated the influence of gold nanoparticle deposition on the overall energetics and catalytic activity of titania.[44,45] Size-dependent quantized conductance at metal nanocontacts has also been demonstrated.[46]

The realization of catalytic properties of ultrasmall gold nanoparticles has led us to probe the size-dependent properties in photocatalytic reactions. Although the metal catalysts have been widely employed in photocatalytic reactions, the influence of particle size on the photoelectrochemical and photocatalytic processes, and their ability to store and transport charge in a semiconductor-metal composite system, is less understood. By isolating the individual charge-transfer steps, we have succeeded in probing the factors that dictate the overall photocatalytic activity of the semiconductor−metal composite system. Furthermore, we have probed the effect of particle size of gold nanoparticles on the charge distribution and Fermi level equilibration of the composite system.

Experimental Section

Synthesis of Metal Nanoparticles. Hydrogen tetrachloroaurate trihydrate, dodecanethiol (DDT), mercaptopropionic acid (MPA), tetraoctylammonium bromide (TOAB), and toluene used in the synthesis of the gold colloids were obtained from Aldrich and used as supplied. A biphasic reduction procedure was adopted to prepare different sized gold nanoparticles.[47−50] TOAB in 7-mL toluene (50 mM) was stirred with the aqueous solution (3 mL) of $HAuCl_4$ (0.04M) for 30 min to transfer $(AuCl_4)^-$ into the organic phase. Reduction with 3-mL $NaBH_4$ solution (0.4 M) produced 8-nm-diameter gold particles. These colloids were then stirred with DDT and MPA to functionalize the surface with thiols.

If we carry out the reduction of $(AuCl_4)^-$ in the presence of dodecanethiol (DDT) and mercaptopropionic acid (MPA), we obtain smaller size gold nanoparticles. For example, by adding 1 mL (0.11 M) solution of dodecanethiol (DDT) and 1 mL (0.11 M) of 3-mercaptopropionic acid (MPA) to the organic phase prior to the addition of $NaBH_4$, we obtain 5-nm-diameter gold nanoparticles. By increasing the concentrations of the two thiols by a factor of 2, we can obtain 3-nm-diameter particles. Thus, by varying the ratio of the thiols:Au we were able to obtain desired size gold particles. While the two thiols (DDT and MPA) were maintained at equimolar concentrations in all these preparations, the Au-to-thiol ratio was altered between 1:4 and 1:2 to prepare 3- and 5-nm-size gold nanoparticles. After the $NaBH_4$ reduction, the colloidal gold solution was further stirred for 30 min following the reduction and then washed repeatedly with dilute acid and deionized water and dried with Na_2SO_4. The final concentration of Au colloids as estimated on the basis of atomic concentration was 13 mM. Unless otherwise indicated, all concentrations in the experiments described below refer to atomic concentrations.

Synthesis of Colloidal TiO_2 Suspension and Nanostructured Films. A colloidal suspension of TiO_2 (0.01 M) was obtained by the addition of 6.25% Ti(IV) isopropoxide in 2-propanol to ethanol under constant stirring. The sol was then diluted with an equal amount of toluene to obtain 5.5 mM TiO_2. To avoid particle growth during extended storage, stock solutions were prepared fresh on a daily basis and used after 2−3 h of aging. The average particle diameter is ∼15 nm. Unless otherwise specified, a 4-mL solvent mixture of 1:1 (v/v) ethanol:toluene was used to suspend gold and TiO_2 nanoparticles.

Nanostructured TiO_2 films were synthesized in an acidic medium by sol−gel technique.[26] The transparent films were cast on a conducting glass electrode by applying the TiO_2 sol followed by air-drying. The films were annealed in air at 673 K for 1 h. By immersing the TiO_2 film in a DDT-MPA modified gold sol for 3 h, we can chemically bind gold nanoparticles to the TiO_2 surface. As described earlier,[40] mercaptopropionic acid (MPA) acts as a bifunctional surface modifier linking carboxylic acid group to TiO_2 and thiol group to gold surface.

Optical and Electrochemical Measurements. Absorption spectra were recorded with a Shimadzu UV-VIS-NIR 3101 PC spectrophotometer. Transmission electron microscopy (TEM) was carried out to determine the sizes of the Au nanoparticles. Specimens were prepared by applying a drop of the gold colloids to a carbon-coated copper grid. Particle sizes were determined from the micrographs recorded at a magnification of 250000× using a Hitachi H600 transmission electron microscope. The photoexcitation of TiO_2 and TiO_2−Au composites was carried out using collimated light from a 150 W xenon lamp filtered through a $CuSO_4$ solution (λ > 300 nm). The electrochemical

(29) Parmon, V. N. *Adv. Hydrogen Energy (Hydrogen Energy Prog.)* **1990**, *8*, 801.
(30) Sharon, M.; Licht, S. Solar Photoelectrochemical Generation of Hydrogen Fuel. In *Semiconductor Electrodes and Photoelectrochemistry*; Licht, S., Ed.; WILEY−VCH: Weinheim, 2002; Vol. 104, p 8920.
(31) Burgeth, G.; Kisch, H. *Coord. Chem. Rev.* **2002**, *230*, 41.
(32) Wood, A.; Giersig, M.; Mulvaney, P. *J. Phys. Chem. B* **2001**, *105*, 8810.
(33) Jakob, M.; Levanon, H.; Kamat, P. V. *Nano Lett.* **2003**, *3*, 353.
(34) Subramanian, V.; Wolf, E. E.; Kamat, P. V. *J. Phys. Chem. B* **2003**, *107*, 7479.
(35) Chen, S.; Murray, R. W. *J. Phys. Chem. B* **1999**, *103*, 9996.
(36) Chen, S.; Ingram, R. S.; Hostetler, M. J.; Pietron, J. J.; Murray, R. W.; Schaaff, T. G.; Khoury, J. T.; Alvarez, M. M.; Whetten, R. L. *Science* **1998**, *280*, 2098.
(37) Hicks, J. F.; Templeton, A. C.; Chen, S.; Sheran, K. M.; Jasti, R.; Murray, R. W.; Debord, J.; Schaaff, T. G.; Whetten, R. L. *Anal. Chem.* **1999**, *71*, 3703.
(38) Hostetler, M. J.; Green, S. J.; Stokes, J. J.; Murray, R. W. *J. Am. Chem. Soc.* **1996**, *118*, 4212.
(39) Ipe, B. I.; George Thomas, K.; Barazzouk, S.; Hotchandani, S.; Kamat, P. V. *J. Phys. Chem. B* **2002**, *106*, 18.
(40) Kamat, P. V.; Barazzouk, S.; Hotchandani, S. *Angew. Chem. Int. Ed.* **2002**, *41*, 2764.
(41) Ung, T.; Dunstan, D.; Giersig, M.; Mulvaney, P. *Langmuir* **1997**, *13*, 1773.
(42) Bamwenda, G. R.; Tsubota, S.; Kobayashi, T.; Haruta, M. *J. Photochem. Photobiol., A* **1994**, *77*, 59.
(43) Haruta, M. *Catal. Today* **1997**, *36*, 153.
(44) Valden, M.; Lai, X.; Goodman, D. W. *Science* **1998**, *281*, 1647.
(45) Yang, Z. X.; Wu, R. Q.; Goodman, D. W. *Phys. Rev. B* **2000**, *6*, 14066.
(46) Li, J.; Yamada, Y.; Murakoshi, K.; Nakatoa, Y. *Chem. Commun.* **2001**, 2170.
(47) Brust, M.; Walker, M.; Bethell, D.; Schffrin, D. J.; Whyman, R. *J. Chem. Soc., Chem. Commun.* **1994**, 801.
(48) Brust, M.; Fink, J.; Bethell, D.; Schiffrin, D. J.; Kiely, C. *J. Chem. Soc., Chem. Commun.* **1995**, 1655.
(49) George Thomas, K.; Zajicek, J.; Kamat, P. V. *Langmuir* **2002**, *18*, 3722.
(50) Leff, D. V.; Ohara, P. C.; Heath, J. R.; Gelbart, W. M. *J. Phys. Chem.* **1995**, *99*, 7036.

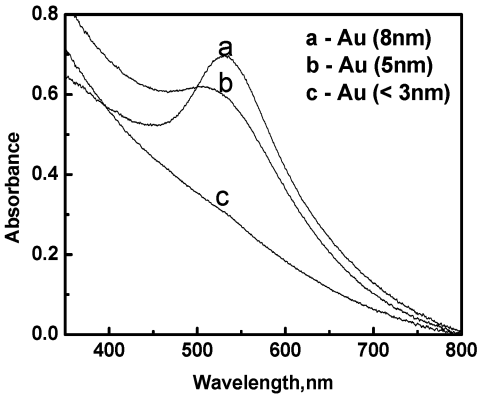

Figure 1. Absorbance spectra of 3-, 5-, and 8-nm Au nanoparticles in toluene. The particle size was varied by controlling the thiol:Au ratio of (a) 4:1, (b) 2:1, and (c) 4:1. For 8-nm size particles, thiols were added after preparing Au nanoparticles (stabilized with TOAB) in toluene suspension.

Scheme 2. Binding of TiO_2 and Au Nanoparticles Using a Bifunctional Surface Modifer

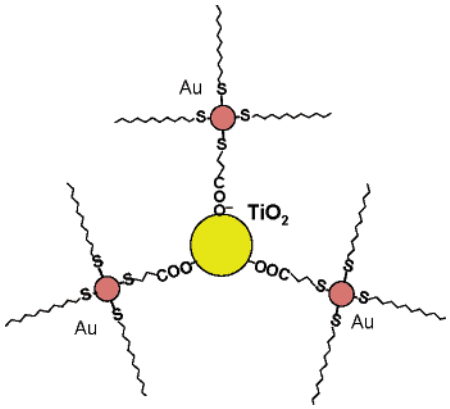

measurements were performed using a PAR Model 173 potentiostat. Nanosecond laser flash photolysis experiments were performed using a Lambda Physik-Laser system (308 nm, output ~10mJ/pulse, pulse width ~10 ns). A typical experiment consisted of a series of 8−10 replicate shots, which were averaged for a single measurement. The details of the experimental setup can be found elsewhere.[51]

Results

Gold Nanoparticles of Different Size. The reduction of $AuCl_4^-$ ions in the presence of tetraoctylammonium bromide yields ~8-nm-diameter gold nanoparticles. These particles can be further derivatized with molecules having SH− or NH_2− functional groups.[12,52,53] For example, gold particles prepared in TOAB/toluene suspension were stirred with the equimolar MPA and DDT to achieve a surface capping of thiols for 8-nm-diameter gold particles. If alkane thiols are added in controlled amounts prior to the biphasic reduction process, we can obtain 3- and 5-nm diameter Au nanoparticles. Whereas DDT functionalization keeps the particles in the organic phase, MPA serves as a linker to bind to TiO_2 surface via −COOH functional group (Scheme 2).

Figure 1 shows the absorption spectra of three Au colloids employed in the present study. The increase in the thiol:Au ratio increases the possibility of surface complexation at early stages, thus arresting the particle growth.[50,54,55] The spectra recorded in Figure 1 show the appearance of plasmon absorption as we increase the particle diameter from 3 to 8 nm. For 5-nm particles, we observe this band as a broad shoulder while a sharper band emerges at 530 nm for 8-nm Au nanoparticles. TEM images of these different size Au nanoparticles are shown in Figure 2**.** The mean diameter estimated from the TEM images are, 3, 5, and 8 nm, respectively. This further supported our strategy of using different Au:thiol ratios for controlling the size. TEM image of Au colloids with 4:1 thiol:Au ratio corresponding to the spectra c in Figure 1 indicated the presence of particles <3-nm diameter. More details on achieving ordered structures using thiol-capped Au nanoparticles can be found elsewhere.[49,56,57]

Accumulation of Electrons in Photoexcited TiO_2 Nanoparticles. UV excitation of TiO_2 colloids in deaerated ethanol-toluene results in charge separation (reactions 1 and 2).[58,59] As the photogenerated holes (h_{VB}) are scavenged by ethanol, the conduction band electrons (e_{CB}) get trapped at Ti^{4+} sites (referred as e_t)

$$TiO_2 + h\nu \rightarrow TiO_2\,(e_{CB} + h_{VB}) \quad (1)$$

$$TiO_2\,(e_{CB} + h_{VB}) + C_2H_5OH \rightarrow TiO_2\,(e_t) + {}^{\bullet}C_2H_4OH \quad (2)$$

Such electron accumulation is marked by the blue coloration of the TiO_2 suspension. Figure 3A shows the absorption spectra of a deaerated colloidal TiO_2 suspension in ethanol:toluene recorded following the excitation with UV light (λ > 300 nm). The blue coloration of the TiO_2 sol is marked by the broad absorption in the visible with a maxima ~675 nm as electrons get trapped at the Ti^{4+} sites. The inset in Figure 3A shows the effect of oxygen on electron accumulation during UV irradiation. The increase in the absorbance at 675 nm is seen only in the absence of oxygen and remains undisturbed upon stopping the illumination. When UV irradiation is carried out in aerated TiO_2 suspension, the photogenerated electrons fail to accumulate as they are scavenged by dissolved oxygen (reaction 3).

$$TiO_2\,(e_{CB} + h_{VB}) + O_2 \rightarrow TiO_2 + O_2^- \quad (3)$$

We have independently determined the concentration of electrons accumulated in the TiO_2 particle using thionine dye as an acceptor. By determining the number of reduced dye molecules, we estimate an accumulation of ~300 electrons per 15-nm TiO_2 particle during extended UV irradiation. (See Supporting Information Part A for further details.)

Charge Equilibration Between TiO_2 and Au Colloids. To probe the charge transfer between TiO_2 and Au colloids, we first transferred 4 mL of TiO_2 suspension in a quartz cuvette capped with a septum. The suspension was purged with N_2 gas and was then subjected to UV illumination for 2 h. The blue coloration of the solution ensured the accumulation of electrons

(51) Thomas, M. D.; Hug, G. L. *Comput. Chem. (Oxford)* **1998**, *22*, 491.
(52) Shipway, A. N.; Katz, E.; Willner, I. *Phys. Chem. Phys.* **2000**, *1*, 18.
(53) Hostetler, M. J.; Templeton, A. C.; Murray, R. W. *Langmuir* **1998**, *15*, 3782.
(54) Henglein, A.; Meisel, D. *Langmuir* **1998**, *14*, 7392.
(55) Henglein, A. *Langmuir* **1999**, *15*, 6738.
(56) Brust, M.; Bethell, D.; Kiely, C. J.; Schiffrin, D. J. *Langmuir* **1998**, *14*, 5425.
(57) Henglein, A.; Meisel, D. *J. Phys. Chem. B* **1998**, *102*, 8364.
(58) Bahnemann, D.; Henglein, A.; Lilie, J.; Spanhel, L. *J. Phys. Chem.* **1984**, *88*, 709.
(59) Kamat, P. V.; Bedja, I.; Hotchandani, S. *J. Phys. Chem.* **1994**, *98*, 9137.

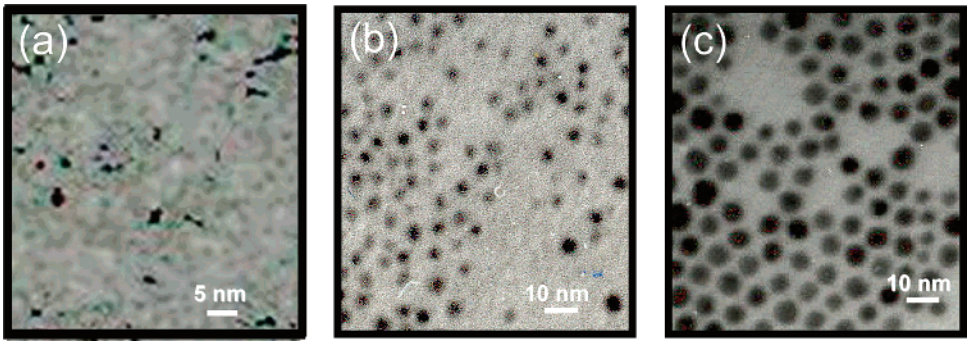

Figure 2. TEM image of Au colloids (a) 3 nm, (b) 5 nm, and (c) 8 nm.

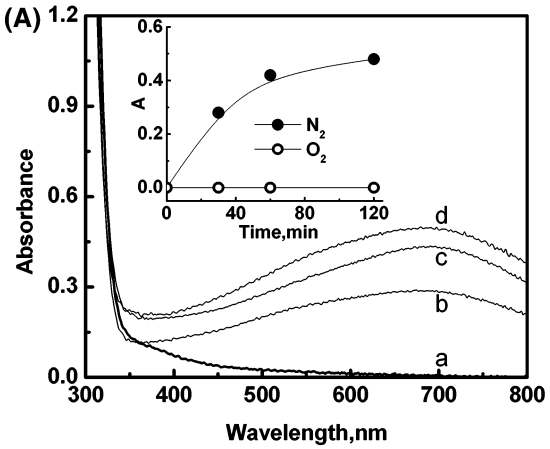

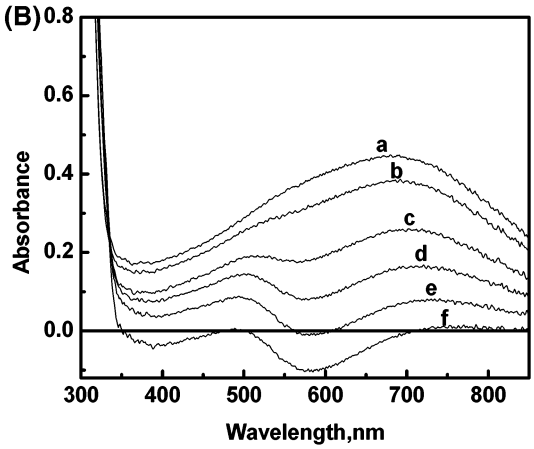

Figure 3. (A) Absorbance spectra of 5.5 mM deaerated TiO_2 suspension in 1:1 (v/v) ethanol-toluene recorded following different periods of UV illumination (λ > 300 nm): (a) 0, (b) 30, (c) 60, and (d) 120 min. Inset shows the effect of O_2 and N_2 on the absorbance change at 675 nm during UV irradiation. (B) Effect of gold nanoparticle addition on the absorption spectra of TiO_2 (5.5 mM) suspension (previously irradiated with UV light (λ > 300 nm) for 120 min). A known amount of deaerated suspension of Au was syringed into the sealed cuvette containing TiO_2 solution (UV irradiated) and the reference cell. The concentrations of Au were (a) 0, (b) 31, (c) 63, (d) 126, (e) 188, and (f) 248 μM of deaerated Au (5-nm diameter).

within the semiconductor particles. The blue color remained unchanged upon stopping the UV illumination. A known amount of 13 mM gold nanoparticle suspension (previously deaerated) was then injected into both the sample and reference cells under N_2 atmosphere. After each addition, the sample was allowed to equilibrate for 5 min and an absorption spectrum was recorded. Figure 3B shows the absorption spectra recorded following the addition of gold nanoparticle suspension to both the reference and sample cells. With successive addition of Au colloids, the

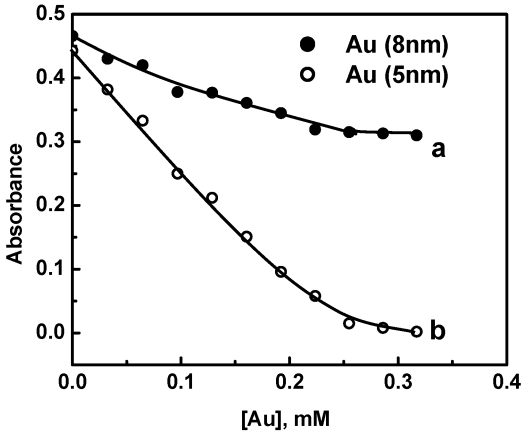

Figure 4. Decrease in the absorbance at 675 nm upon addition of Au suspension (deaerated) containing (a) 8-nm and (b) 5-nm-diameter particles. The TiO_2 suspension was deaerated and UV irradiated prior to the addition of Au nanoparticles.

peak at 675 nm decreases as the accumulated electrons in the TiO_2 are transferred to Au nanoparticles. At higher Au concentrations, we also observe bleach around 550 nm in the difference absorption spectrum. This is likely to be caused by the dampening of the Au plasmon band as electrons are accumulated within the gold particles.

Since the absorption in the visible region is indicative of the electron concentration remaining in TiO_2 nanoparticles, we followed the absorption changes at 675 nm following the addition of different amounts of Au nanoparticles. Figure 4 shows the decrease of the absorbance at 675 nm at different concentrations of 5- and 8-nm gold nanoparticles. For the same concentration of Au (as presented in terms of atomic concentration), 5-nm particles are more effective than the 8-nm particles. For any given gold (Au^0) concentration, we expect 4−5 times greater concentration of 5-nm particles than 8-nm particles. As a greater number of small Au nanoparticles interact with charged TiO_2 particles, we observe an enhanced disappearance of blue color by the smaller size particles. In most of our experiments, we employed relatively low concentration of Au particles (particle concentration ratio of Au:TiO_2 as 1:1 or less). If we compare the 675-nm absorbance decrease at constant particle concentration, we observe 8-nm particle as better quenchers. This in turn indicates that a greater number of electrons are necessary to achieve charge equilibration with 8-nm Au particle than 5-nm Au particle. (The potential change associated with single-electron transfer is smaller for larger Au particle than for the smaller particle.) These results are illustrated in the Supporting Information Part B.

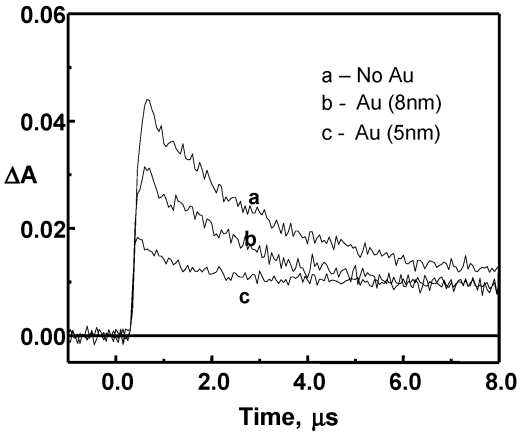

Figure 5. Transient decay observed at 800 nm following 308-nm laser excitation of deaerated 5.5 mM TiO_2 solution containing (a) no Au, (b) 126 μM Au (8 nm), and (c) 126 μM Au (5 nm).

Transient Absorption Studies. If indeed the decrease in blue color is associated with electron transfer to Au particles, we should be able to probe this event using time-resolved absorption spectroscopy. The charge transfer between TiO_2 and Au colloids was probed by monitoring the transient absorption decay at 675 nm following 308-nm laser pulse excitation of a deaerated TiO_2 solution (Figure 5). Band gap excitation of TiO_2 colloid using UV−laser pulse causes charge separation followed by charge recombination and charge-trapping processes. Characterization of electron-trapping events in TiO_2 colloids has been done earlier using picosecond and femtosecond laser flash photolysis.[60−64] The prompt appearance of a transient absorption in trace a (Figure 5) indicates that electron trapping is completed within the laser pulse duration of 10 ns. This result is in accordance with earlier observation that the electron trapping is completed within 30 ps.[60] The decay of the absorbance in the microsecond time scale represents the fraction of electrons that are lost in the recombination process.

When the laser flash photolysis experiments of TiO_2 colloids were carried out in the presence of 5- and 8-nm Au nanoparticles, we observed a decrease in the maximum absorbance immediately following the laser pulse (traces b and c in Figure 5). The decrease in the maximum absorbance is an indication that fewer electrons remain in the TiO_2 particles. The difference in the maximum absorbance observed in the absence and presence of Au colloids corresponds to the amount of electrons that reside in the Au nanoparticles. Tthe 5-nm Au nanoparticles show greater decrease in the maximum absorbance than that observed with 8-nm Au nanoparticles. This observation parallels the steady-state observations presented in Figure 4.

The absorption−time profiles shown in Figure 5 also indicate that the charge distribution between the gold and the photoexcited TiO_2 nanoparticles is completed within the laser pulse duration. Experiments are currently underway to time-resolve the interparticle electron transfer in the subnanosecond time scale. Close examination of the initial decay fraction reveals that the charge recombination is significantly decreased in the presence of gold nanoparticles. The transfer of electrons from

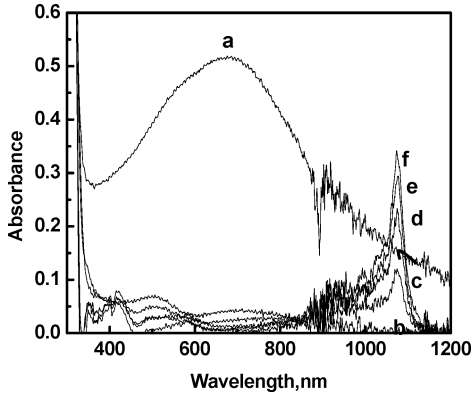

Figure 6. Absorption spectra of deaerated TiO_2 (5.5 mM) suspension after UV irradiation (λ > 300 nm) for 120 min: (a) before and (b) after addition of 0.6 mM Au nanoparticles (8-nm diameter). After equilibrating TiO_2 and Au system, known amounts of C_{60} solution (deaerated) was syringed into the sample and reference cells. The concentrations of C_{60} in the sample cell were (c) 5.9, (d) 11.7, (e) 17.5, and (f) 23.2 μM.

TiO_2 to gold nanoparticle is expected to suppress the charge recombination process. As will be discussed later in this paper, the improved charge separation in TiO_2−Au nanocomposite is important in maximizing its photocatalytic performance. (Because of the limitation in the time window, we are not able to comment on the long-term electron accumulation in the absence and presence of gold nanoparticles.)

Au Mediated Reduction of C_{60} in UV-Irradiated TiO_2 Suspensions. C_{60}/C_{60}^- redox couple is a convenient probe for determining the Fermi level of semiconductor particles.[33] C_{60}^- is stable in N_2 atmosphere and is readily monitored from its absorption maximum at 1075 nm. In the present study, we probed the C_{60}^- formation during the one-electron transfer from UV-excited TiO_2 to C_{60} (Reaction 4).[59]

$$TiO_2\,(e) + C_{60} \rightarrow TiO_2 + C_{60}^- \qquad (4)$$

In a typical experiment, the TiO_2 colloids were excited with UV light for 60 min. The deaerated C_{60} solution was then added in small increments to the preirradiated TiO_2 suspension. An equal amount of C_{60} was also added to the reference cell before recording the absorption spectra. The increased absorption at 1075 nm confirms the formation of C_{60}^-. The reduction (reaction 4) continues until the C_{60}/C_{60}^- redox couple equilibrates with the TiO_2 (e) system.

We systematically probed the Au-mediated electron transfer to C_{60} by introducing Au nanoparticles first into the UV-irradiated TiO_2 suspension. The spectra *a* and *b* in Figure 6 were recorded before and after the addition of Au particles to the UV-irradiated TiO_2 suspension. As discussed in the previous section, the decreased blue coloration shows the transfer of electrons to Au nanoparticles as the two particles undergo charge equilibration (Reaction 5). If indeed, most of the electrons reside within the gold nanoparticles in the TiO_2/Au composite, we should be able to extract these electrons in a reductive process. In other words, if we introduce C_{60} to the TiO_2/Au composite system, we would expect gold nanoparticles to mediate the reduction of C_{60} (Scheme 3). Accordingly, when we add C_{60} solution to the equilibrated TiO_2/Au(e) suspension (viz., the solution corresponding to spectrum *b*), we observed the absorption band with a maximum at 1075 nm (spectra *c*−*f* in Figure 6**)**. This increase in 1075-nm absorption quantitatively represents

(60) Serpone, N.; Lawless, D.; Khairutdinov, R.; Pelizzetti, E. *J. Phys. Chem.* **1995**, *99*, 16655.
(61) Serpone, N.; Lawless, D.; Khairutdinov, R. *J. Phys. Chem.* **1995**, *99*, 16646.
(62) Sant, P. A.; Kamat, P. V. *Phys. Chem. Chem. Phys.* **2002**, *4*, 198.
(63) Evans, J. E.; Springer, K. W.; Zhang, J. Z. *J. Chem. Phys.* **1994**, *101*, 6222.
(64) Colombo, D. P. J.; Bowman, R. M. *J. Phys. Chem.* **1995**, *99*, 11752.

Scheme 3. Stepwise Transfer of Electrons from TiO_2 to Au to C_{60} Following the Excitation of TiO_2 Particle

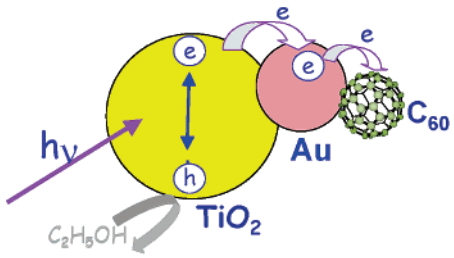

the formation of C_{60}^- as a result of electron transfer (reaction 6).

$$TiO_2\,(e) + Au \rightarrow TiO_2{-}Au\,(e) \qquad (5)$$

$$TiO_2{-}Au\,(e) + C_{60} \rightarrow TiO_2{-}Au + C_{60}^- \qquad (6)$$

The absorption at 1075 nm increases with increasing concentration of C_{60}, finally attaining saturation as the C_{60}/C_{60}^- redox couple equilibrates with the electrons accumulated in the TiO_2/Au composite system. Although noble metal mediated photocatalytic reduction reactions have been demonstrated before (see, for example, references 5 and 6), the present experiments provide, for the first time, a systematic approach to isolate the individual electron-transfer steps (viz., TiO_2 (e) → Au (e) → C_{60}^-). The ability to probe such individual electron-transfer steps is an important aspect toward understanding the factors that dictate the noble metal mediated catalytic reduction processes.

Formation of C_{60}^- Using Laser Pulse Excitation. C_{60} radical anion formation was time-resolved in a laser flash photolysis experiment using 308-nm laser pulses as the excitation source and monitoring the transient absorption growth at 1075 nm. C_{60} was introduced into the deaerated TiO_2 and TiO_2/Au suspensions before subjecting them to the 308-nm laser pulse excitation. The identity of the C_{60} anion was also confirmed by recording the transient absorption spectra following 150 μs after laser pulse excitation **(**Figure 7A**)**. Absorption−time profiles recorded under same experimental conditions are shown in Figure 7B. The distinct signature of C_{60} anion formation with a maximum at 1075 nm is observed only in the presence of TiO_2 and TiO_2−Au suspensions. The absorbance at maximum seen in traces *d* is significantly higher than that of trace c (Figure 7A), thereby confirming the increased yield of C_{60} anion in the TiO_2/Au composite system. Blank experiments carried out with the excitation of gold suspension alone or with C_{60} show negligibly small absorption at 1075 nm (traces *a* and *b* in Figure 7A and 7B).

Figure 8 shows the formation of C_{60}^- in a TiO_2/Au suspension following the laser pulse excitation. The saturation in the absorption growth seen around 150 μs shows the time scale at which we achieve equilibration between the TiO_2/Au composite and the C_{60}/C_{60}^- redox couple. The maximum absorbance attained at 150 μs increased with increased C_{60} concentration. The increased yield of C_{60}^- confirmed the ability of C_{60} to extract electrons from the TiO_2−Au composite system (reaction 6), in agreement with the steady-state experiments discussed in Figure 6. The absorption−time profiles shown in Figure 8

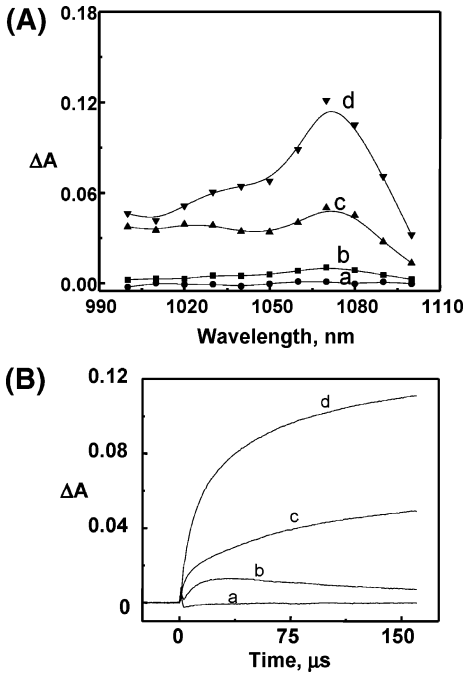

Figure 7. (A) Difference absorption spectra and (B) absorption−time profiles at 1075 nm recorded following the 308-nm excimer laser pulse excitation of deaerated toluene:ethanol (1:1 v/v) solution containing (a) 0.2 mM Au (8-nm diameter), (b) 0.2 mM Au (8-nm diameter) and 12 μM C_{60}, (c) 5.5 mM TiO_2 with 12 μM C_{60}, and (d) 5.5 mM TiO_2 with 0.2 mM Au (8-nm diameter) and 12 μM C_{60}.

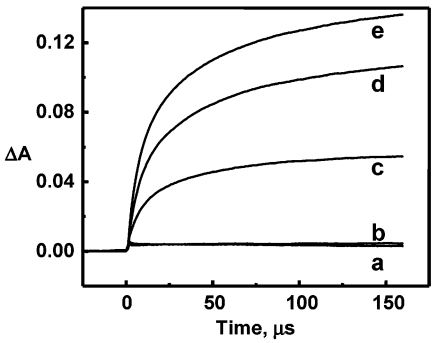

Figure 8. Transient absorption−time profile recorded at 1075 nm following the 308-nm laser pulse excitation in a deaerated solution containing (a) 5.5 mM TiO_2, (b) 5.5 mM TiO_2 and 0.2 mM Au (8-nm diameter). Traces c−e indicate the formation of C_{60} anion with increasing C_{60} concentration in a suspension containing 5.5 mM TiO_2 and 0.2 mM Au (8 nm): (c) 6, (d) 12, and (e) 18 μM C_{60}.

represent the time scale with which C_{60} extracts electrons and undergoes equilibration with the TiO_2−Au composite system.

Discussion

The stepwise reduction achieved in the steady-state and laser flash photolysis experiments confirm the mediating role of Au nanoparticles toward storing and shuttling electrons in a TiO_2-assisted photocatalytic reduction process. The increased yield of C_{60}^- in the photocatalysis experiment illustrates the catalytic role that a noble metal plays toward enhancing the efficiency of interfacial charge-transfer process.

The Fermi level (E_F) of the semiconductor is directly related to the number of accumulated electrons as illustrated in the expression 7.

$$E_F = E_{CB} + kT \ln n_c/N_c \qquad (7)$$

Scheme 4. Equilibration of Semiconductor−Metal Nanocomposites with the Redox Couple before and after UV Irradiation

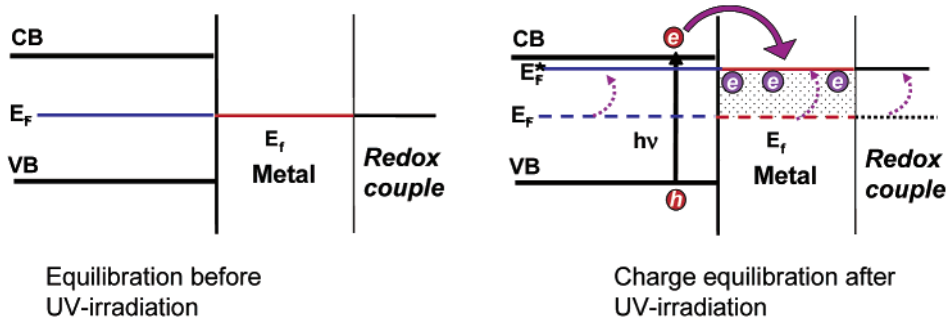

Table 1. Apparent Fermi Level of TiO_2 and TiO_2/Au Nanocomposite Systems

photocatalyst	diameter of Au particle (nm)	$[C_{60}]_0$ (μM)	$[C_{60}^-]^a$ (μM)	E_F^{*b} (mV)
TiO_2		94	36.1	−230 mV
TiO_2−Au	8	94	50.9	−250 mV
TiO_2−Au	5	94	65.6	−270 mV
TiO_2−Au	3	94	76.8	−290 mV

[a] A suspension containing 5.5 mM TiO_2 and 0.06 mM Au in 1:1 toluene: ethanol mixture was irradiated with UV light for 30 min. Equilibrated concentration of C_{60}^- was determined spectrophotometrically after the addition of concentrated C_{60} solution to the preirradiated suspension. [b] $E_F^* = E_{fb} = -0.25 + 0.059 \log [C_{60}]_{eq}/[C_{60}^-]$ where $[C_{60}]_{eq} = [C_{60}]_0 - [C_{60}^-]$.

E_{CB} is the conduction band energy level versus NHE, n_c is the density of accumulated electrons, and N_c is the charge carrier density of the semiconductor. If we accumulate more electrons in the TiO_2 or TiO_2−Au system, we would expect a negative shift in the Fermi level of the TiO_2. By shifting the Fermi level closer to the conduction band, it would therefore be possible to improve the energetics of the semiconductor system.

In the present investigation, we determined the apparent Fermi level of the semiconductor particle by attaining a Nernstian equilibrium with a known redox couple (viz., C_{60}/C_{60}^-). The apparent Fermi level (E_F^*) was correlated to the concentration of the redox species by using expression 8,[33,65,66]

$$E_F^*(TiO_2\ (e)) = E_{fb} = E^\circ_{Ox/Red} + 0.059 \log([Ox]_{eq}/[Red]_{eq}) \quad (8)$$

where E_F^* and E_{fb} are the apparent Fermi level and the flat band potential of TiO_2 (or TiO_2/Au) and $E^\circ_{Ox/Red}$ is the standard reduction potential of the redox couple (viz., $E^\circ(C_{60}/C_{60}^{\bullet -})$ −0.25 V versus NHE). By determining the equilibrium concentration of C_{60}^- in the UV-irradiated TiO_2 and TiO_2/Au suspension from the absorption at 1075 nm ($\epsilon = 16\,000\ M^{-1}\ cm^{-1}$), we can obtain the values of E_F^* (expression 8).

The experiments were carried out by mixing the known concentration of deaerated TiO_2 and Au particles first and then irradiating the composite clusters for 30 min with UV light. A known amount of deaerated C_{60} solution was injected into the preirradiated suspension and the equilibrium concentration of C_{60}^- was determined from the absorbance at 1075 nm. The apparent Fermi level for TiO_2 and TiO_2/Au systems determined from expression 8 are summarized in Table 1. In the absence of a noble metal, we obtain an apparent Fermi level value of −230 mV versus NHE for TiO_2 particulate system. (This value is about 270 mV more positive than the conduction band of bulk TiO_2 at neutral pH.) However, when the TiO_2 particles are in contact with Au nanoparticles, we observe a negative shift in the Fermi level. The apparent Fermi level as determined for TiO_2/Au system were −250, −270, and −290 mV for 8-, 5-, and 3-nm size gold nanoparticles, respectively. This shift of Fermi level to more negative potential is the result of a higher degree of electron accumulation causing the composite system to be more reductive than the pristine TiO_2 system.

Murray and co-workers have demonstrated that Au nanoparticles possess the property of storing electrons in a quantized fashion.[35,36] The double-layer charging around the metal nanoparticle facilitates storage of the electrons within the gold nanoparticle. When the semiconductor and metal nanoparticles are in contact, the photogenerated electrons are distributed between TiO_2 and Au nanoparticles (Fermi level of Au = +0.45 V versus NHE). The transfer of electrons from the excited TiO_2 into Au continues until the two systems attain equilibration. Since the electron accumulation increases the Fermi level of Au to more negative potentials, the resultant Fermi level of the composite shifts closer to the conduction band of the semiconductor. This observed shift in the Fermi level of the composite system is in agreement with the earlier observation for the ZnO−Au systems.[32,34] The negative shift in the Fermi level is an indication of better charge separation and more reductive power for the composite system. Scheme 4 illustrates the shift in the Fermi level of the composite as a result of charge equilibration between semiconductor and metal nanoparticles.

Another interesting observation in Table 1 is the particle size effect on the shift of apparent Fermi level. The smaller Au particles induce greater shift in E_F^* than the larger particles. For example, −60 mV shift in flat band potential was achieved using 3-nm-diameter gold nanoparticles as compared to −20 mV shift for 8-nm Au nanoparticles. This shows that we can tune the apparent Fermi level of the composite system by controlling the size of the metal nanoparticle. Since the energy levels in the gold nanoparticles are discrete, we expect a greater shift in the energy level for each accumulated electron in smaller size Au nanoparticles than the larger ones. For example, a shift of 0.1 V/electron has been reported for ~2 nm Au nanoparticles.[36] Thus, the composite catalyst with smaller Au nanoparticles is expected to be more active catalytically than that composed of larger Au particles. These observations parallel the size-dependent catalytic properties of gold nanoparticles deposited on titania in earlier studies.[43] By probing the photoinduced electron-transfer process in a systematic way, we have now succeeded in demonstrating the effect of gold nanoparticle size on the overall energetics of the TiO_2−Au composite system.

(65) Nenadovic, M. T.; Rajh, T.; Micic, O. I.; Nozik, A. J. *J. Phys. Chem.* **1984**, *88*, 5827.
(66) Dimitrijevic, N. M.; Savic, D.; Micic, O. I.; Nozik, A. J. *J. Phys. Chem.* **1984**, *88*, 4278.

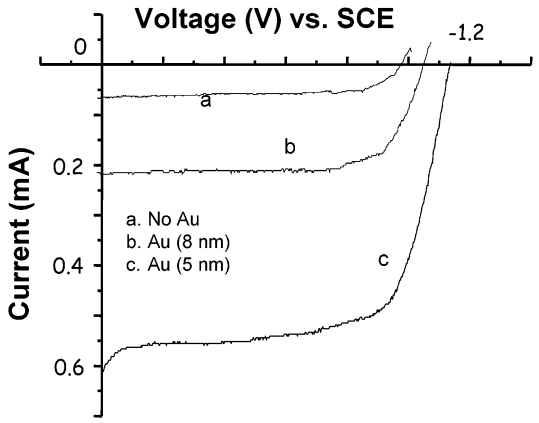

Figure 9. I−V characteristics of (a) TiO_2, (b) TiO_2/Au (8-nm diameter), and (c) TiO_2/Au (5-nm diameter) composite film. Measurements were performed in a three-arm cell with Pt as counter electrode, a saturated calomel electrode as reference, and 3-mL 0.05 M NaOH as electrolyte. UV light from xenon lamp ($\lambda > 300$ nm) was used as the excitation source.

If indeed, such a particles size effect influences the energetics by shifting the Fermi level to more negative potentials, we should be able to translate this beneficial effect to the photoelectrochemistry of nanostructured semiconductor films. To confirm this effect, we deposited TiO_2 and TiO_2−Au films on conducting glass electrodes as described in the Experimental Section and used them as photoanode in a photoelectrochemical cell. A 0.05 M NaOH solution was used as the electrolyte. Photocurrents at different applied potentials were recorded under UV illumination. The current−voltage characteristics are presented in Figure 9. The zero-current potential in these traces correspond to apparent flat band potential of the nanostructured semiconductor film. At this applied potential, all the photogenerated electrons and holes recombine without producing any net current flow. Any built-in driving force within the film for driving electrons to the collecting surface of OTE is neutralized by the applied negative bias. Thus, we can use the value of zero-current potential to compare the flat band potential (or apparent Fermi level) of TiO_2 films that are modified with different size Au nanoparticles.

From Figure 9 it is evident that the apparent flat band potential of nanostructured TiO_2 in 0.05 M NaOH is at −0.98 V versus SCE (trace a). A shift in the flat band potential to negative potentials is seen for the TiO_2−Au composite system. The shifted apparent flat band potential is observed at −1.04 V and −1.14 V versus SCE for electrodes modified with 8- and 5-nm gold nanoparticles, respectively. In other words, we can still draw a significant photocurrent using the TiO_2/Au system at potentials (e.g., −0.98 V vs SCE) that show complete recombination in pristine TiO_2. Obviously, the presence of Au facilitates charge separation and promotes interfacial electron transfer at the electrolyte interface. The trend of size-dependent shift of flat band potential is similar to that obtained in the particle suspension system (Table 1). (The difference in the medium pH and the morphology of the composite renders the absolute values of E_F* different.) The improved photoelectrochemical performance is also reflected in the net photocurrent generation. The observed photocurrents at positive bias are significantly higher for the composite films involving Au nanoparticles. These photoelectrochemical measurements further confirm the effect of noble metal in improving the energetics of the semiconductor nanostructures.

Conclusions

Charge equilibration between photoirradiated TiO_2 and Au nanoparticles has been probed to elucidate the photocatalytic activity of semiconductor−metal nanocomposites. Such a charge distribution between the two systems has a direct influence on the energetics of the composite by shifting the Fermi level to more negative potentials. The greater shift in the Fermi level observed with smaller Au nanoparticle is reflected in greater photocatalytic reduction efficiency and higher photocurrent generation. The present study provides mechanistic explanation for the size-dependent catalytic activity of Au nanoparticles in the TiO_2/Au composite. By carrying out sequential electron transfer from TiO_2 to Au to C_{60}, we have for the first time isolated the individual charge-transfer steps that dictate a photocatalytic process. A better understanding of the mediating role of metal nanoparticle is important for designing next-generation photocatalysts for light-energy conversion.

Acknowledgment. The work described herein was supported by the Office of the Basic Energy Sciences of the U.S. Department of Energy. We would like to thank Dr. Dan Meisel for helpful discussions. This is contribution No. 4496 from the Notre Dame Radiation Laboratory.

Supporting Information Available: Experimental details and discussion related to the determination of electron concentration in TiO_2 and TiO_2/Au particles (Part A) and electron redistribution between TiO_2 and Au at constant particle concentration (Part B) (PDF). This material is available free of charge via the Internet at http://pubs.acs.org.

JA0315199